

# Visual Appearance of Waterwall Tube Failures Due to Hydrogen Damage Mechanism in Coal Fired Power **Plants**

Deepak Kumar Gope, Anil Kumar Das, Prahlad Halder\*

Advanced Materials Research Lab, NTPC Energy Technology Research Alliance, NTPC Ltd., Greater Noida, Uttar Pradesh, India.

\*prahladhalder@ntpc.co.in

#### Abstract

Failures of boiler tubes in coal fired power plant are due to unforeseen reasons are a major concern to power engineers. Out of different failure mechanisms, hydrogen damage is one of the corrosion related mechanisms assisted by high temperature that occurs predominantly in water wall tubes of the subcritical boiler. The general physical appearance of a water wall tube failure on account of Hydrogen Damage is "Window Opening". This paper highlights two other distinct failure appearances associated with hydrogen damage, and their appearance exhibits as "Slit Type" and "Puncture type" opening. It is also observed that hydrogen damage may occur both in relatively new units with only a few years of services and in older plants. Micro-fissures observation in optical microscopy is one of its key assertive features. The study also showed that the failure was intergranular in nature. Based on the evidences, it was observed that the failure was high temperature hydrogen induced under deposit corrosion in nature.

Keywords: Hydrogen damage, water wall tube, micro-fissures, under deposit corrosion

#### 1 Introduction

Coal-fired power plants play a vital role in the energy sector due to their ability to provide reliable and large-scale power generation. Despite the growing emphasis on renewable energy sources, thermal power plants remain essential for meeting global energy demands [1]. The main components of a thermal power plant include the boiler, turbine, generator, condenser, and cooling system. Among them boiler is considered to be the heart of a coal-fired power plant. The primary function of a boiler is to produce steam at the desired pressure and temperature by converting the chemical energy stored in the fuel (primarily coal) into heat energy [2]. This steam acts as the working fluid for the power cycle and is essential for the turbine's operation. Power plant boilers are generally categorized into major four types – (a) Subcritical, (b) Supercritical, (c) Ultrasupercritical, and (d) Advanced ultra-supercritical boiler, based on operating pressure and temperature. A subcritical boiler operates at 17.2 MPa pressures which is below the critical point of water (22.1 MPa) [3]. A boiler is basically a large pressure vessel consisting of large number of tubes and pipes. All the four sides of boiler are fabricated by panels of hundreds of tubes. Boiler tubes mainly consist of water walls, economiser, reheater and superheater tubes depending on the different heat zones of the boiler. The water wall tube in a boiler is a series of closely spaced tubes (usually made of carbon steel or low alloy steel) that form part of the boiler's furnace walls. In subcritical boilers, water and steam exist in separate phases, and steam is produced through the phase change of water into steam in the evaporator section which mainly consists of water wall tubes. Boiler tubes are among the most failure-prone components due to exposure to extreme heat and pressure. General boiler tube failure damage mechanisms are overheating, creep, erosion, hydrogen damage, stress corrosion cracking, pitting, flow accelerated corrosion, fatigue failure, thermal fatigue and welding related failures.

In general, failures of the water wall tubes are on account of different factors such as ash accumulation, corrosion and overheating etc. Hydrogen damage is one of the corrosion-related phenomena. It is basically an under-deposit corrosion mechanism at elevated temperature in which metals become susceptible to embrittlement due to the absorption of hydrogen atoms [4]. Hydrogen damage is a broader term which includes different mechanism leading to the failure of the components. It includes low temperature hydrogen embrittlement, high temperature hydrogen attack, hydrogen induced blistering, hydrogen induced cracking and hydride formation [5]. Low temperature hydrogen embrittlement refers to the loss of ductility and/or the formation of cracks in metals or alloys due to the presence of atomic hydrogen, typically at low temperatures. It can occur in various forms, depending on the material properties, manufacturing processes, and environmental conditions. It includes both irreversible embrittlement and cracking that may occur during manufacturing, before the component is put into service, as well as damage that develops during actual service. High-Temperature Hydrogen Attack (HTHA) is a permanent and irreversible degradation of a metal's mechanical properties due to exposure to hydrogen at elevated temperatures. Unlike corrosion or erosion, HTHA is an internal damage mechanism. It does not cause visible wall thinning or large-scale deformation, making it harder to detect without detailed inspection techniques [5, 6]. Hydrogen damage occurs when hydrogen atoms diffuse into the metal lattice, often during high-temperature operations or exposure to corrosive environments, leading to a significant reduction in the material's ductility and strength [7]. The atomic hydrogen when combined with carbon in steel at elevated temperatures and pressures, results in the formation of methane gas along the ferrite grain boundaries [8–11].

The locations of the hydrogen damage failure are confined to the water wall tubes in power plant components. This phenomenon can occur in wide spectrum of material grade like carbon steel, austenitic stainless steel, Aluminium, magnesium etc. depending on the working environment [6].

In majority of the existing literatures, hydrogen damage failures are predominantly characterized by a classical window-type opening appearance [4,9,12]. In this paper three case studies were taken from three different subcritical boilers with different ages of thermal power plants. This paper discusses about the visual appearance of hydrogen damage mechanism in boiler components. It includes slit type opening and puncture

type opening apart from window type opening. Through three distinct case studies, authors provide a comprehensive illustration of these varied failure appearances of hydrogen damage which is rarely available in the existing literature. It also provides some preventive measures of hydrogen damage.

## 2 Methodology

The present study analyzed three failed samples collected from boilers of varying capacities and service durations. The detail of the sample is presented in table 1. In all the cases, failures occurred in the water wall section which is in the high heat flux zone of the boiler. From table 1, it can be observed that the power rating of the thermal power plant is from 110 MW to 500 MW and all the plants have subcritical boiler. The 110 MW power plant operates at  $\sim$ 13-15 MPa pressure and  $\sim$ 537-543°C temperature. The 250 MW boiler operates at a pressure of  $\sim$ 15-17MPa and 537-543°C temperature while the 500 MW boiler operates at a pressure of  $\sim$ 17-19 MPa and 537-543°C temperature.

#### 2.1 Visual observation

Visual observation of the samples was carried out by unaided eye and stereo microscope (make M/s Leica). Images were captured using Nikon D70S camera. Figure 1 showed the images of the as received samples. Fig 1 (a & b) represents sample number 1 which is a window type opening failure. This sample was taken from 110 MW power plant. Fig 1 (c & d) shows sample no. 2 which is a puncture type opening and taken from a 250 MW power plant. Fig 1 (e, f & g) illustrate the images of sample no. 3 which was failed from a 500 MW boiler.

Sample No.	Plant Capacity (MW)	Plant Age (Years)	Dimension of sample (OD X T) in mm Away from Failure	Visual appearance
1	110	24	63.5 X 6.3	Window type opening (WTO)
2	250	8	63.2 X 7.6	Puncture type opening (PTO)
3	500	31	57.5 X 7	Slit type opening (STO)

Table 1. Details of the samples taken for case study

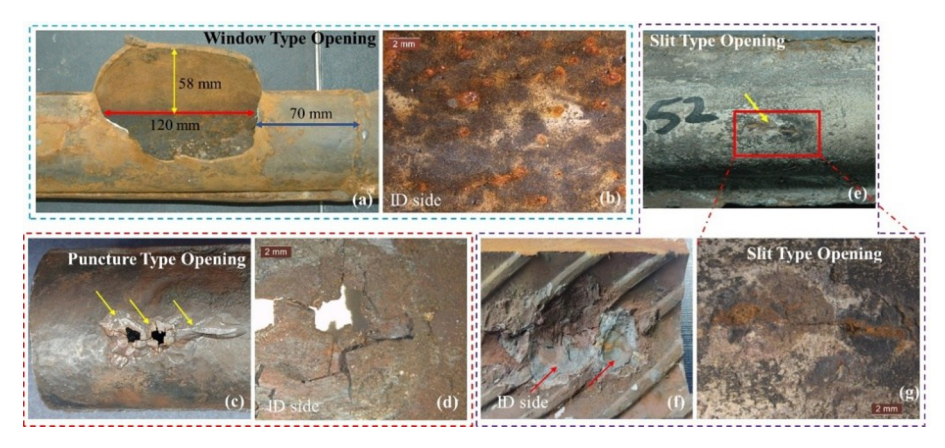


**Fig. 1.** (a) As received tube showed window type opening failure near to the weld joint; (b) ID side of the tube showed pitting and corrosion; (c) As received tube showed puncture type opening with two punctures and sever erosion marks around it; (d) ID side of the tube after sectioning showed oxide layer and its spallation around the crack; (e) The sample tube showed slit type opening at OD (Outside Diameter) side of the tube; (f) ID side of the tube showed under deposit corrosion in localised region with crater of iron oxide; (g) Magnified view of the tube at marked location showed short and intact crack having length ~25 mm.

## 2.2 Chemical composition

The chemical analysis of all the samples was carried using Optical Emission Spectrometer (OES) method (Make: M/s Thermofischer scientific, ARL 3460). Before chemical analysis, the samples were grinded to obtained a flat and smooth area of minimum dimension of 12 x 12 mm<sup>2</sup>.

## 2.3 Microstructure and hardness analysis

For microstructural study purpose, small specimens from selected locations of all the samples were taken using precision abrasive cutting machine (to avoid heating) and mounted for suitable edge retention. All the mounted specimens were subjected to multiple stages of grinding & polishing to obtain a mirror finish surface. The last stage of polishing operation is carried out using specific cloth suitable for 0.5-1 µm diamond paste. These metallographic specimens were studied under optical microscope (Make: M/s Leica microsystem, DMi8) with un-etched and etched conditions. Etching of the samples were done using 2% Nital solution. After metallographic study, the mould samples are taken for micro hardness analysis using Vickers micro hardness tester (Make: M/s Tinius Olsen) with a load of 0.5 kgf using a diamond indenter.

## 3 Results

## 3.1 Sample no. 1

The sample tube was failed as window type opening. The failure was at a distance of 70 mm from the circumferential welding as indicated in fig 1 (a). The opening was  $\sim$ 58 mm wide and 120 mm in length. The thickness of the tube at fracture edge was  $\sim$ 4 mm. The side of the tube opposite to the failure did not show any damage. However, the inner wall of the tube opposite to failure showed corrosion and pitting which is shown in fig. 1(b).

Microstructure showed multiple cracks originating from internal surface. The length of these cracks varies from 0.22 mm to 1.17 mm. Magnified view (fig. 2b) of indicated location showed numerous intergranular micro fissures and degraded structure. Fracture edge also showed numerous micro-fissures as can be observed in fig 2c. Microhardness at failed location was in the range of 124 – 137 HV0.5.

## 3.2 Sample no. 2

The as received tube sample showed two punctures having circular appearance (approx. dia 3 mm). Sever thinning and erosion marks were observed around the failed location. The dip erosion mark was ~26 mm in length along the longitudinal direction of the tube. Magnified view of external surface of the failed location showed multiple cracks around the punctures. The sample was sectioned to open the tube for study of its internal surface. The internal surface at failed location showed under deposits corrosion & spallation of oxide layer. The side opposite to failed location showed no failure.

Microstructure at failed location showed thick oxide layer of thickness  $\sim 1.76$  mm at ID side of the tube. It also showed sever thinning at fracture edge. Tube thickness at failed location was  $\sim 1$  mm. The magnified view at fracture edge showed numerous micro fissures. Microhardness at failure location was in the range of 172 - 175 HV 0.5.

#### 3.3 Sample no. 3

The water wall tube showed tightly intact crack. The crack was  $\sim 25$  mm in length. The tube was sectioned to observe the internal surface at failed location. The inner surface showed under deposit corrosion with crater of iron oxide. Thinning of the tube at failed location was also observed. Thickness of tube at failure was  $\sim 3.3$  mm while the thickness of the tube away from the failure was 7 mm.

Microstructure at failed location shows through crack of width 330  $\mu m$  with thick oxide layer of thickness ~1.4 mm at ID side of the tube. It showed numerous micro fissures around the cracks. Microstructure showed ferritic & pearlite structure with intergranular micro-fissures. Microhardness values at failed location were in the range of 147 – 150 HV0.5.

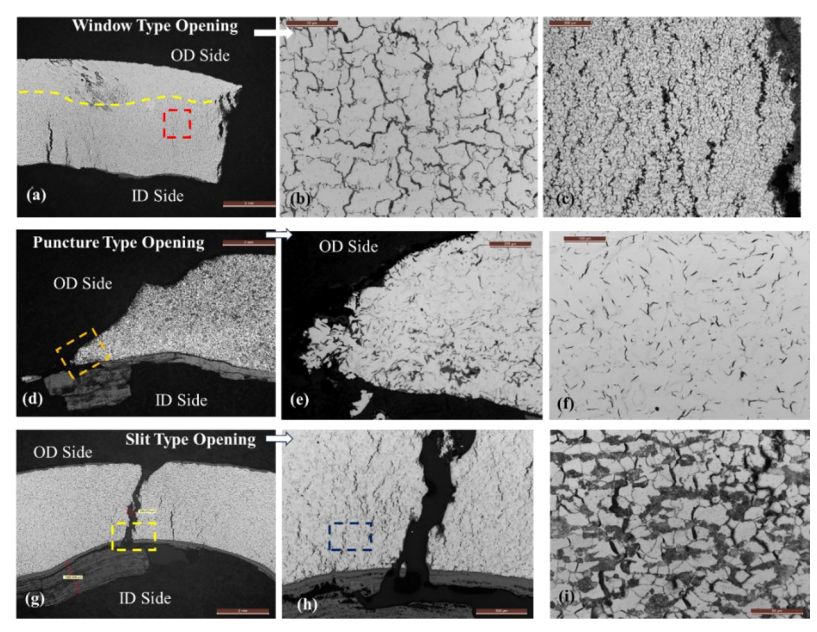


Fig 2. (a) Microstructure for sample no. 1 showed multiple cracks originating from internal surface. The crack length varies from 0.22 mm to 1.17 mm. The yellow dotted line showed the extend of micro fissures from ID side (Unetched condition) (feature at top left side is polishing error); (b) Magnified view at fracture edge (marked by red dotted box in fig a) showed numerous micro-fissures. (Unetched condition); (c) Microstructure at fracture edge, showed numerous intergranular micro fissures. (Etched condition) and decarburization; (d) Microstructure for Sample no. 2 showed thick oxide layer at ID side of the tube (etched condition); (e) At fracture edge, micro-fissures and oxide filled cracks observed (Unetched condition) (Magnification: 50X marked by orange dotted box); (f) At fracture edge (unetched condition) microstructure showed micro-fissures, (Magnification: 200X); (g) Microstructure for sample no. 3 showed thick oxide layer and through crack; (h) Microstructure showed numerous micro fissures on both side of the crack; (i) Microstructure showed numerous intergranular micro fissures.

Steel grade (%)  $\mathbf{C}$ Si Mn S 0.35 0.10 0.035 0.035 0.29 - 1.06SA210 Gr. C[13] Max Min Max Max Sample no. 1 0.24 0.18 0.005 0.013 0.54 (110MW)Sample no. 2 0.24 0.21 0.74 0.0050.011 (250 MW) Sample no. 3 0.29 0.20 0.91 0.0036 0.019 (500 MW)

Table 2. Chemical composition and other details of the samples.

## 3.4 Chemical Analysis

The Chemical composition of all the tube samples obtained through OES analysis are shown in table 2.

## 4 Discussion

Hydrogen damage is a broad term associated with material degradation due to interaction of hydrogen with material. In this degradation, the material loses its ductility and strength. Waterwall tubes in coalfired power plant carries water and/or steam. When there is a deviation in water chemistry, it may lead to under deposit corrosion. The deposit creates a barrier between the water and the metal surface, causing localized heat retention and reduced heat transfer. Beneath the deposits, water decomposition at high temperatures initiates corrosion reactions that generate atomic hydrogen (H). This atomic hydrogen diffuses into the metal, reacting with Fe<sub>3</sub>C (iron carbide) at the grain boundaries to form CH<sub>4</sub> (methane) which have high volume fraction of methane [6,14] results in micro fissures.

The location of water wall tube is in the high heat flux zone of the boiler. In sample no. 2 (250 MW boiler) the failure occurred in a period of 8 years' time as mentioned in table 1. Contrast to this, the third case (500 MW boiler) which was in service for more than 30 years. Thus, hydrogen damage failure is independent of year of service. Whenever, the water chemistry was compromised it results in corrosion which may subsequently leads to hydrogen damage.

The samples were sectioned from the failure location and prepared for metallurgical analysis as discussed in methodology part. When the polished samples were examined under an optical microscope, numerous micro-fissures were observed. These fissures were clearly visible in unetched condition which is one of the key microstructural features of hydrogen damage.

The slit type opening is very localized as compared to WTO and PTO type failure appearance. The affected area in the form of micro-fissures is most prominent in the WTO mode and extends to nearly 81% of the tube thickness at the fracture edge. Complete decarburization of pearlite was observed in WTO mode. Also, there is no significant reduction in thickness of tube material at fracture edge as compared to sample no. 3 (STO). The possible reason for thickness reduction in sample no. 3 is the extent of under deposit corrosion. The thickness of under deposit oxide layer at failure in this sample was ~1.4 mm. No comparison regarding thickness reduction can be made for PTO sample, as external steam erosion on the OD side of the tube has influenced the measurement. Therefore, the overall assessment of failure modes should consider multiple contributing factors, including: (a) affected areas, (b) area of under deposit corrosion, (c) thickness reduction due to under deposit corrosion, (d) temperature

influence at the heat flux region, (e) dimension of the component and operating temperature and pressure.

Higher hydrogen concentrations significantly increased the tendency for intergranular (IG) cracking while the transgranular mode of cracking was evident at lower hydrogen pressure [15]. A brittle fracture is typically associated with IG-type failure[16]. However, it may be inferred that micro fissures regions are the indication of amount of hydrogen absorption. In all the three samples, the rupture of tubes was due to the formation and linkage of micro-fissures which is a typical signature of hydrogen damage mechanism. Intergranular mode of failure was predominant in all the three samples.

Remedial Mechanism for Hydrogen Damage. Once water wall tube failure was detected due to hydrogen damage, suitable corrective action should be taken to minimize loss of power generation which includes (a) thickness survey across the affected region, (b) Replace all the affected tubes, (c) Assessment of deposit analysis and corrective measures as per OEM guidelines, (d) Corrosion mapping and (e) NDT technique like UT (Ultrasonic Testing) and Eddy current. This is important because, even though localized, the failures would be found in most of the adjacent tubes. The preventive measures that the power plant should follow in order to avoid loss of power generation due to hydrogen damage are as follow:

- Boiler water chemistry parameters recommended by OEM/Plant should be maintained to avoid internal deposition
- During overhauling or maintenance location prone for deposition to be assessed to avoid any significant under deposit corrosion.
- Periodic assessments to be carried out for deposit analysis as per standard guidelines & accordingly suitable action to be taken.

#### 5 Conclusion

Based on the analysis of all the three case studies of different capacity of subcritical boilers following conclusion can be drawn:

- i. The failure appearance of hydrogen damage can also be manifested as "Puncture-type opening" or "Slit-type opening" apart from "Window-type openings.
- ii. Hydrogen damage phenomenon is localised in nature as observed in the boiler tubes and it may happen within very short span of time to years old service if water chemistry is not maintained properly.
- iii. The failure of the water wall tubes was attributed to under-deposit corrosion phenomenon, which creates an environment for ionization of hydrogen and its diffusion into the base metal under high temperature and pressure. Therefore, the nature of failure of all the three tubes was high temperature hydrogen induced under deposit corrosion.
- iv. A key microstructural feature was the presence of micro-fissures which is intergranular in nature.

- v. The possible reasons for different appearance of failure were affected areas with micro fissures, thickness reduction, extent of under deposit corrosion, temperature, pressure and geometry of the components.
- vi. Based on this study, it may be inferred that the reason for WTO was that the affected areas on account of micro-fissures were very high as compared to STO & PTO type.
- vii. It might be inferred that metallographic technique is very reliable & confirmative method for failure of tube due to hydrogen damage.

**Acknowledgments.** Authors would like to express their gratitude to the Executive Director of NTPC NETRA for strong motivation for writing this paper. This work was not supported by any funding agency.

**Disclosure of Interests.** The authors declare that they have no conflicts of interest to disclose regarding the research presented in this manuscript.

## References

- [1] V.K. Yadav, M. Fulekar, M.H. Fulekar, The current scenario of thermal power plants and fly ash: production and utilization with a focus in India, International Journal of Advance Engineering and Research Development 5 (2018). https://www.researchgate.net/publication/329942803.
- [2] I. Dincer, Y. Bicer, Fundamentals of energy systems, Integrated Energy Systems for Multigeneration (2020) 33–83. https://doi.org/10.1016/B978-0-12-809943-8.00002-9.
- [3] A.A. Nuraini, S. Salmi, H.A. Aziz, Efficiency and Boiler Parameters Effects in Subcritical Boiler with Different Types of Sub-bituminous Coal, Iranian Journal of Science and Technology Transactions of Mechanical Engineering 44 (2020) 247–256. https://doi.org/10.1007/s40997-018-0249-7.
- [4] James J Dillon, Paul B Desch, Tammy S Lai, The Nalco Guided to Boiler Failure Analysis, second edition, 2011.
- [5] K. Poorhaydari, A Comprehensive Examination of High-Temperature Hydrogen Attack—A Review of over a Century of Investigations, J Mater Eng Perform 30 (2021) 7875–7908. https://doi.org/10.1007/s11665-021-06045-z.
- [6] X. Li, X. Ma, J. Zhang, E. Akiyama, Y. Wang, X. Song, Review of Hydrogen Embrittlement in Metals: Hydrogen Diffusion, Hydrogen Characterization, Hydrogen Embrittlement Mechanism and Prevention, Acta Metallurgica Sinica (English Letters) 33 (2020) 759–773. https://doi.org/10.1007/s40195-020-01039-7.
- [7] M. Moshtaghi, B. Loder, M. Safyari, T. Willidal, T. Hojo, G. Mori, Hydrogen trapping and desorption affected by ferrite grain boundary types in shielded metal and flux-cored arc weldments with Ni addition, Int J Hydrogen Energy 47 (2022) 20676–20683. https://doi.org/10.1016/J.IJHYDENE.2022.04.260.
- [8] M. Djukic, G. Bakic, M. Djukic, V. Sijacki Zeravcic, G. Bakic, D. Milanovic, B. Andjelic, Model of Influencing Factors for Hydrogen Damages of Boiler Evaporator Tubes, n.d. https://www.researchgate.net/publication/236612261.

- [9] M.B. Djukic, V. Sijacki Zeravcic, G.M. Bakic, A. Sedmak, B. Rajicic, Hydrogen damage of steels: A case study and hydrogen embrittlement model, Eng Fail Anal 58 (2015) 485–498. https://doi.org/10.1016/j.engfailanal.2015.05.017.
- [10] R.A. Oriani, The diffusion and trapping of hydrogen in steel, Acta Metallurgica 18 (1970) 147–157. https://doi.org/10.1016/0001-6160(70)90078-7.
- [11] Y.S. Chen, C. Huang, P.Y. Liu, H.W. Yen, R. Niu, P. Burr, K.L. Moore, E. Martínez-Pañeda, A. Atrens, J.M. Cairney, Hydrogen trapping and embrittlement in metals A review, Int J Hydrogen Energy (2024). https://doi.org/10.1016/j.ijhydene.2024.04.076.
- [12] Y.S. Kim, W.C. Kim, J. Jain, E.W. Huang, S.Y. Lee, Hydrogen Embrittlement of a Boiler Water Wall Tube in a District Heating System, Metals (Basel) 12 (2022). https://doi.org/10.3390/met12081276.
- [13] ASTM, Standard Specification for Seamless Medium-Carbon Steel Boiler and Superheater Tubes, in: ASTM A210/A210M-19, 2019: p. 03.
- [14] S. Lynch, Discussion of some recent literature on hydrogen-embrittlement mechanisms: addressing common misunderstandings, Corrosion Reviews 37 (2019) 377–395. https://doi.org/10.1515/corrrev-2019-0017.
- [15] Y. Ogawa, D. Birenis, H. Matsunaga, O. Takakuwa, J. Yamabe, Ø. Prytz, A. Thøgersen, The role of intergranular fracture on hydrogen-assisted fatigue crack propagation in pure iron at a low stress intensity range, Materials Science and Engineering: A 733 (2018) 316–328. https://doi.org/10.1016/j.msea.2018.07.014.
- [16] E.D. Merson, P.N. Myagkikh, V.A. Poluyanov, D.L. Merson, A. Vinogradov, Features of the Hydrogen-Assisted Cracking Mechanism in the Low-Carbon Steel at Ex- and Insitu Hydrogen Charging, in: Procedia Structural Integrity, Elsevier B.V., 2018: pp. 1141–1147. https://doi.org/10.1016/j.prostr.2018.12.238.

**Open Access** This chapter is licensed under the terms of the Creative Commons Attribution-NonCommercial - NoDerivatives 4.0 International License (http://creativecommons.org/licenses/by-nc-nd/4.0/), which permits any noncommercial use, sharing, distribution and reproduction in any medium or format, as long as you give appropriate credit to the original author(s) and the source, provide a link to the Creative Commons license and indicate if you modified the licensed material. You do not have permission under this license to share adapted material derived from this chapter or parts of it.

The images or other third party material in this chapter are included in the chapter's Creative Commons license, unless indicated otherwise in a credit line to the material. If material is not included in the chapter's Creative Commons license and your intended use is not permitted by statutory regulation or exceeds the permitted use, you will need to obtain permission directly from the copyright holder.

